




Article

# A Novel Application of Computational Contact Tools on Nonlinear Finite Element Analysis to Predict Ground-Borne Vibrations Generated by Trains in Ballasted Tracks

Andrés García Moreno <sup>1</sup>, Antonio Alonso López <sup>2</sup>, María G. Carrasco García <sup>1</sup> , Ignacio J. Turias <sup>3</sup>   
and Juan Jesús Ruiz Aguilar <sup>1,\*</sup> 

<sup>1</sup> Department of Industrial and Civil Engineering, Algeciras School of Engineering and Technology (ASET), University of Cádiz, 11202 Algeciras, Spain; andres.garciamoreno@uca.es (A.G.M.); maria.carrasco@uca.es (M.G.C.G.)

<sup>2</sup> Independent Researcher, Palo Alto Numerics, 28031 Madrid, Spain; antonio.alonso.lopez@gmail.com

<sup>3</sup> Department of Computer Science Engineering, Algeciras School of Engineering and Technology (ASET), University of Cádiz, 11202 Algeciras, Spain; ignacio.turias@uca.es

\* Correspondence: juanjesus.ruiz@uca.es

**Abstract:** Predictive numerical models in the study of ground-borne vibrations generated by railway systems have traditionally relied on the subsystem partition approach (segmented). In such a method, loads are individually applied, and the cumulative effect of the rolling stock is obtained through superposition. While this method serves to mitigate computational costs, it may not fully capture the complex interactions involved in ground-borne vibrations—especially in the frequency domain. Recent advancements in computation and software have enabled the development of more sophisticated vibrational contamination prediction models that encompass the entire dynamics of the system, from the rolling stock to the terrain, allowing continuous simulations with a defined time step. Furthermore, the incorporation of computational contact mechanics tools between various elements not only ensures accuracy in the time domain but also extends the analysis into the frequency domain. In this novel approach, the segmented models are shifted to continuous simulations where the nonlinear problem of a rigid–flexible multibody system is fully considered. The model can predict the impact of a high-speed rail (HSR) vehicle passing, capturing the key intricacies of ground-borne vibrations and their impact on the surrounding environment due to a deeper comprehension of the occurrences in the frequency domain.

**Keywords:** HSR; railway; ground-borne vibrations; vibrational emissions; prediction; FEM; numerical modelling; computational contacts



**Citation:** Moreno, A.G.; López, A.A.; Carrasco García, M.G.; Turias, I.J.; Ruiz Aguilar, J.J. A Novel Application of Computational Contact Tools on Nonlinear Finite Element Analysis to Predict Ground-Borne Vibrations Generated by Trains in Ballasted Tracks. *Modelling* **2024**, *5*, 1454–1468. <https://doi.org/10.3390/modelling5040075>

Academic Editors: Paolo Todisco and Elide Natri

Received: 25 July 2024

Revised: 25 September 2024

Accepted: 30 September 2024

Published: 7 October 2024



**Copyright:** © 2024 by the authors. Licensee MDPI, Basel, Switzerland. This article is an open access article distributed under the terms and conditions of the Creative Commons Attribution (CC BY) license (<https://creativecommons.org/licenses/by/4.0/>).

## 1. Introduction

Railway transportation is regarded as the most sustainable means of moving passengers and cargo in modern society. The advent of high-speed railways (HSRs) has transformed the landscape of railway travel in recent decades, with freight logistics increasingly integrating rail as a core component. This shift is driven by environmental concerns and economic efficiencies. However, railway systems, despite their numerous advantages, generate ground-borne vibrations that can have significant impacts on their surrounding environment. These vibrations originate from the wheel–rail contact, and propagate through track components, subgrade, and soils, affecting surrounding nearby structures [1].

The sources of vibration effects include quasi-static rolling stock moving loads, deformations induced by wheel and/or rail unevenness, punctual track defects, axles passing by, and other track components. To predict vibrations accurately, it is crucial to define the transmission medium between the source and receiver. In addition, a comprehensive analysis of wave propagation and potential attenuation involves examining not only the

time domain but also the frequency domain. Geometrical attenuation, influenced by the distance between the source and measurement point, is unrelated to the frequency domain. On the other hand, material typology attenuation, influenced by the properties of traversed materials, is directly associated with the frequency response [2]. Nevertheless, predicting and assessing these ground-borne vibrations is paramount, especially when planning new railway lines or expansions, as these vibrations can profoundly impact human well-being, particularly within the frequency range of 15 to 200 Hz [3].

Two predominant families of prediction models exist, distinguished by their underlying calculation methods: analytical and numerical. These models diverge in terms of the mechanisms they incorporate to simulate excitation (e.g., quasi-static axle loads, parametric excitation, transient excitation due to rail joints and wheel imperfections, and excitation stemming from wheel and rail irregularities) and their approach to modelling dynamic structure–soil interactions [4]. In this work, a range of relevant studies were analyzed in order to build the base of the state-of-the-art of latest-generation numerical prediction models for ground-borne vibrations.

Initial findings and studies of prediction models assumed homogeneity in the track direction for the ground and structures. By combining Boundary Element Method (BEM) and Finite Element Method (FEM) models to reduce computational efforts, some researchers sought to further enhance the analysis [5]. Other researchers have introduced an all-encompassing 3D Boundary Element Method (BEM) model designed to assess soil motion and the effects of high-speed train (HST) passage on both surface and underground structures, facilitating complete coupling between the soil and adjacent structures. Nevertheless, it is important to highlight that this method heavily depends on environmental factors, leading to an extensive simplification of track elements. This oversimplification may lead to a lack of detailed information concerning events occurring within the track [6].

These kinds of vibrations are intricately linked to various operational factors, such as the condition of the infrastructure, the train speed, and the use of adjacent areas. Primarily, ground-borne vibrations stem from the metallic contact between the train wheels and rail. Critical to numerical predictions in this domain is the selection of an appropriate method to represent wheel and rail unevenness. Various methods have been explored in relevant literature to incorporate them as an additional source of realistic vibrations in prediction models [7,8]. Without these considerations, the resulting signals may lack fidelity.

After conducting this analysis, the decision was made to adopt the standardized representation [9] from various options presented in the literature for addressing such irregularities. This approach was deemed the optimal choice for ensuring reproducibility. In addition to developing the track model, careful attention must be given to defining the representation of the rolling stock. It is essential not only to create a representative model but also to ensure its stability in calculations and realism by incorporating genuine characteristics of the rolling stock. Having identified references that provide detailed descriptions of a 3D rigid–flexible multibody system [10], the modeling process can benefit from a thorough understanding and incorporation of the nuances involved.

Load simulations are generally modeled as a birth-and-death system that includes loads that are punctual and time-dependent [11]. Models must be designed based on the calculation time step to accommodate loads at existing nodes. Loads are distributed as triangular pulses between three nodes. As loads are modeled and vibrations propagate through the tracks and into the ground, they inevitably affect the foundations of nearby structures. Typically, the intensity of ground vibrations diminishes as one moves further from the railway track [12].

There are many types of vibration-prediction models and load simulations, depending on the degree of vehicle modeling and the desired level of representation of the track and environment. In [13], a schematic and detailed summary of these types is presented, with the references cited therein analyzed, identifying those of interest for the detailed modeling of rolling stock and the 3D representation of the track and environment using FEM. It is precisely in this latter case where the fewest reference works are found. Other researchers [14]

employ computational contact techniques at the core of their investigation to represent wheel–rail interactions, including unevenness. The main difference is the consideration of simplifications by assuming linear calculations, which assumes the invariance of the system matrices. Additionally, another approach introduces an explicit modelling method [15], with the introduction of point forces through the use of springs.

All these numerical models were developed and published to serve as the foundation for the present discussion and to highlight the potential implications of these advancements in the field of railway track engineering for effectively controlling vibration emissions. The primary objective of this paper is to introduce and validate a numerical Finite Element (FE) model based on a 3D spatial framework. This model has the versatility to accommodate a wide range of variations along the railway track, thereby enabling a comprehensive understanding of the vibration dynamics. It is important to note that the model will focus on the analysis of vibrations in the immediate proximity of the source, the rail. The goal is to precisely characterize the vibrational signal across the entire track system, allowing for the identification and potential redesign of specific segments with attenuation objectives as needed.

The proposed model incorporates computational contact tools to simulate the transmission of waves throughout the entire train-track system seamlessly, effectively eliminating discontinuities in the application of loads [2,11]. Working with a 3D model and a small time step of 1024 calculations per elapsed second (emulating field measurements with piezoelectric accelerometers), as well as the use of computational contact theories, allows for the continuous introduction of solicitations and the acquisition of a sufficiently dense FFT spectrum up to 512 Hz. This advancement not only enhances time-domain accuracy but also improves the frequency-domain data that can be predicted.

Furthermore, the main novelty lies in simulating a continuous model from the rolling stock to the track. This enables the representation of complex dynamic phenomena, such as those arising from the connections between the carriages of the rolling stock in their complete longitudinal composition and their kinematic motion linkages, which could not be simulated using decoupled models like load-overlay models. By employing this innovative approach, this research aims to contribute to the field of railway engineering by offering a robust framework for assessing and mitigating ground-borne vibrations. This framework is particularly valuable during the infrastructure design and planning stages, as it empowers decision makers to proactively address the potential impact of railway-induced vibrations on sustainability and the quality of life for nearby communities.

## 2. Experimental Data

The genesis of ground-borne vibrational prediction models stemmed from the imperative need for a foundational dataset, serving as a reference benchmark for model development. This underscores the necessity for any subsequent model to have an initial reference point or a reliable comparison framework for calibration and result validation. At this juncture, a fundamental reference for the calibration and validation of such vibrational models can be found in [4]. The study presents measurements from an actual railway track, using accelerometers to monitor a high-speed rail (HSR) line with a double-track configuration, considering the rail, sleeper, ballast, and terrain. In this model, the scenario of a train traveling at 300 km/h was specifically chosen as the most representative of a high-speed rail (HSR) line.

In the particular case presented in [4], the Brussels–Paris HSR line was monitored as a conventional ballast track, as illustrated in Figure 1. The layered structure of the track and subgrade system consists of the following components:

- Subgrade: The foundation layer of the railway system, representing the ground beneath the track.
- Subballast: Positioned above the subgrade, this layer acts as an intermediary component between the subgrade and ballast.

- Ballast: The layer in which the track is embedded, providing essential support and vibration dampening.
- Sleepers: Components strategically placed along the track, supporting the rails and distributing loads.
- Under-Rail Pad: A crucial element for vibration isolation, positioned between the rail and sleeper.
- Rail: The track element that interacts directly with the rolling stock.

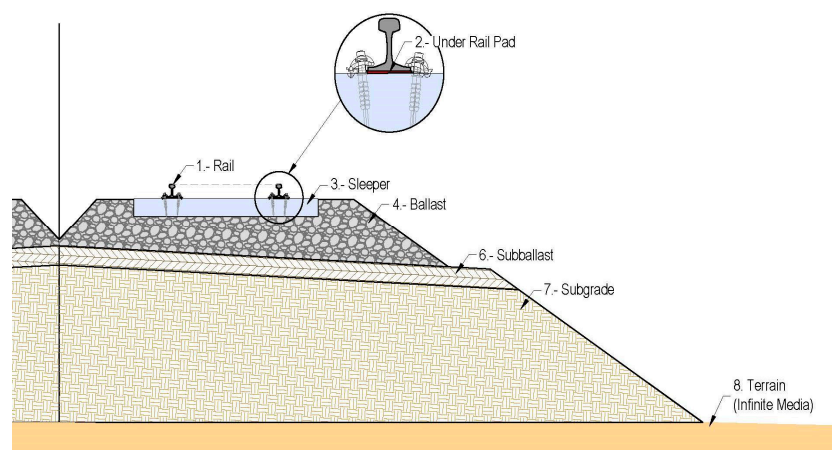


**Figure 1.** Typical cross-section of a high-speed railway and its main components.

Each of these components is defined by a series of inherent characteristics, specific properties that describe the behavior of each material and its response to various conditions, ultimately influencing the transmission of ground-borne vibrations generated by the passage of rolling stock over them. Subsequently, the paper outlines the key characteristics of each component used in [4]. In the proposed study, this assumption is crucial for developing a finite element model that accurately simulates the actual behavior of the materials and components related to the high-speed rail (HSR) line studied in the previously cited research.

The track features continuously welded UIC 60 rails, each with a mass-per-unit length of 60 kg/m and a moment of inertia ( $I$ ) of  $3038 \times 10^{-6} \text{ m}^4$ . These rails are affixed using a Pandrol E2039 rail fixing system onto precast, prestressed concrete monoblock sleepers measuring 2.5 m (m) in length, 0.285 m in width, and 0.205 m in height (under the rail), with a mass of 300 kg.

Flexible rail pads with a thickness ( $t$ ) of 0.01 m and a static stiffness of approximately 100 MN/m, suitable for loads ranging from 15 to 90 kN, are positioned under the rail. The track is supported by a 30 cm layer of ballast, followed by a layer of limestone or porphyry (subballast), and finally, a limestone supporting layer (subgrade).

In addition, the measurements obtained from [4] were conducted during the passage of a Thalys–Alstom high-speed train (Spanish Renfe S100), which in this study serves as the model load. Figure 2 displays the arrangement of the Thalys high-speed train (HST), comprising two locomotives and eight carriages, with a total train length of 200.18 m. Each locomotive is supported by two bogies and is equipped with four axles. In proximity to the locomotives, adjacent carriages share a bogie, while the remaining six carriages share bogies with neighboring ones. This brings the total number of bogies to 13, resulting in a train with a total of 26 axles.

Moreover, Table 1 provides a summary of key parameters, including the axle mass ( $M_u$ ), bogie mass ( $M_b$ ), car mass ( $M_c$ ), primary and secondary stiffnesses ( $k_1$  and  $k_2$ ), and primary and secondary damping coefficients ( $C_1$  and  $C_2$ ) obtained from [16].

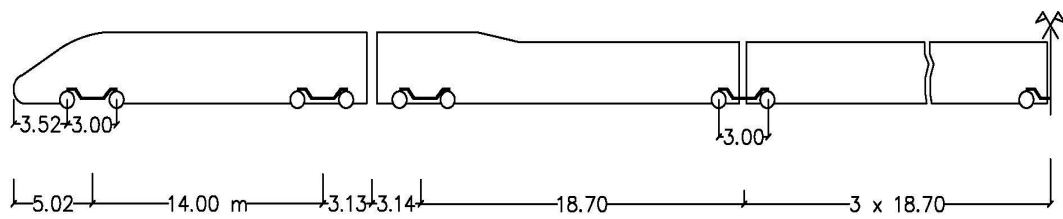


Figure 2. Thalys–Alstom–Renfe S100 high speed train (dimensions in meters) [4].

Table 1. Reference rolling stock [16]. Summary of key parameters.

	$M_u$ (Kg)	$M_b$ (Kg)	$M_c$ (Kg)	$k_1 \times 10^6$ (N/m)	$K_2 \times 10^6$ (N/m)	$C_1 \times 10^3$ (N s/m)	$C_2 \times 10^3$ (N s/m)
Traction car	2048	2380	55,790	2.45	20	2.45	40
Side car	2003	3040	24,000	1.40	10	0.82	48
Central car	2003	3040	24,000	1.40	10	0.82	48

This initial stage of our investigation drew upon data obtained from the literature, encompassing the current state of numerical models and actual measurements from the track. The subsequent stages of the process involved the development, calibration, and validation of the model against on-site measurements using the comparison method. This method primarily entails the graphical comparison of the obtained results with the measured ones for assessment. This calibration process is essential to ensure the accuracy and reliability of our model in replicating real-world ground-borne vibrations.

In the subsequent sections, the developed numerical model is revealed in detail, and the implications of this research are analyzed within the context of railway engineering.

### 3. Materials and Methods: Numerical Model

The proposed model is a Finite Element Method (FEM) model of a layered approach (presented in Figure 1) to represent the subgrade and track system accurately in a 3D environment, as shown in Figure 3. The FEM model generated in this work represents and incorporates all of the components described in Section 2, defining these components with the actual characteristics and properties of the railway infrastructure and superstructure to be modelled.

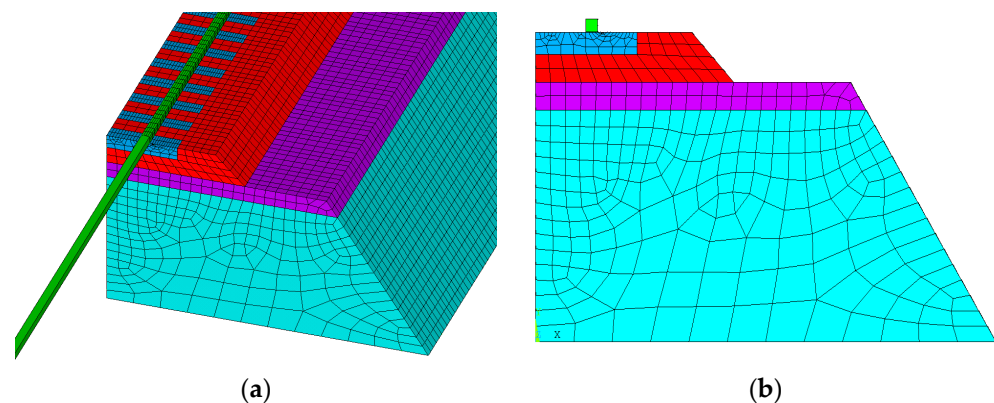


Figure 3. Proposed Finite Element Model of the track and subgrade system: (a) oblique view of the model; (b) cross-section of the model.

To perform the dynamic analysis of the railway system, a general multibody analysis approach is employed, in which two important points need to be considered:

- Formulation of the equations of motion:

The equations of motion (described in Section 3.3) govern the translational and rotational motions of the rolling stock and track elements. These equations consider the forces generated by the train's weight distribution, wheel–rail interactions, and the response of the track components to external loads.

The discrete equations of the system (both flexible and rigid parts), corresponding to the conservation of linear momentum, are obtained following the standard displacement approach in FEM. These equations are completed by adding the constraint equations associated with the joints that connect different bodies.

- Time integration of the equations of motion:

The Newmark method (described in Section 3.4) is the time-integration method used because of its simplicity and proven capacity to capture transient dynamic responses accurately.

By incorporating these mathematical formulations and computational techniques, the model can provide a comprehensive representation of the complex dynamics involved in ground-borne vibrations induced by railway operations. In the subsequent subsections, a detailed explanation of all the subsystems that compose the entire model and their fundamental equations is described.

### 3.1. Railway System and Terrain

The spatial framework of our model is meticulously designed to simulate distinct layers that capture the behavior of the railway track and its surroundings as shown in Figure 3. The structural components of the railway system and the adjoining subgrade undergo meticulous representation through the utilization of solid continuum elements, specifically employing eight-node hexahedron elements. Given the assumed constitutive behavior of linearity, isotropy, and compressibility, a pure displacement formulation is employed to accurately capture the dynamic response of the system. Contact interactions between different parts are modelled using surface-to-surface contact by target and contact elements. Geometric contact detection is performed over target elements, and the role of the contact elements is to provide the points of contact.

The contact algorithm used is the augmented Lagrangian method [17]. Frictionless contact with sliding and separation is considered between the sleepers and ballast, bonded contact between the under-rail pads and sleepers and rail, and separation without sliding contact between the rolling stock wheels and rail.

- Wheel to rail: To simulate the interaction between the rolling stock and rail, non-glued computational contacts are programmed. These contacts allow for the dynamic interaction between the train and track, accounting for factors such as wheel–rail interaction forces and rail irregularities.
- Rail to sleeper: The connection between the rail and sleeper is modelled using a “glued contact”. This modelling technique replicates the effect of the fastening system, ensuring that the rail and sleeper act as a cohesive unit in response to dynamic forces.
- Infinite media: The ground is modelled as an infinite media. To prevent wave reflections that could distort the results, this infinite medium is designed to be wave-absorbent. The simulation employs both linear and viscous damping, following the approach outlined in [18], where damping elements introduce the shear and normal components of ground forces along its boundary. These calculations are based on ground data inputs, specifically the velocities of P-waves and S-waves, which are dependent on the mechanical properties of the soil.

The properties of the track and soil are detailed in Table 2.

Figure 4 illustrates a side view of the contacts between wheel and rail and rail and sleeper through the under-rail pad.

**Table 2.** Parameters of track, embankment, and soil rolling stock, with the following values: Young’s modulus (E), Poisson’s ratio ( $\nu$ ), and density ( $\rho$ ).

Element	E (Pa)	$\nu$	$\rho$ (Kg/m <sup>3</sup> )
Rail	$2.10 \times 10^{11}$	0.3	$2.92 \times 10^3$
PAD	$1.00 \times 10^8$	0	65.24
Sleeper	$7.15 \times 10^{10}$	0.25	$2.5 \times 10^3$
Ballast	$1.45 \times 10^8$	0.2	$1.9 \times 10^3$
Subballast	$1.25 \times 10^8$	0.3	$1.9 \times 10^3$
Embankment	$1.40 \times 10^8$	0.3	$2.0 \times 10^3$
Infinite media	$1.20 \times 10^8$	0.3	$1.6 \times 10^3$

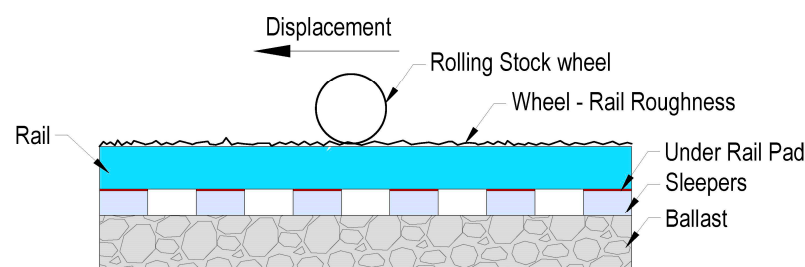


**Figure 4.** Side view representation of vehicle–track systems interaction.

### 3.2. Rolling Stock

The rolling stock is modelled as a rigid multibody system. Each rigid part is a compound of a pilot node, which drives the motions of the rest of nodes of the rigid body. Bodies are connected to each other through joints, imposing kinematic constraints between the two nodes they connect. Additionally, spring-damper elements are introduced between bodies to model the suspension system, as shown in Figure 5.

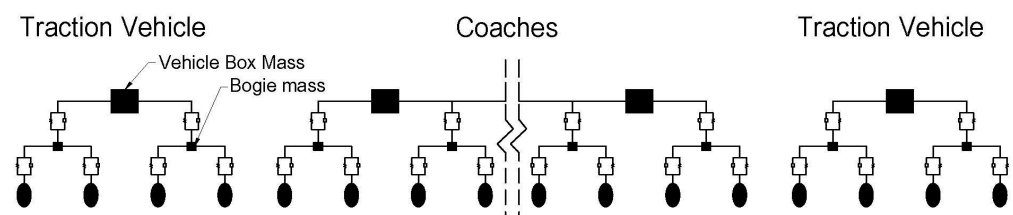


**Figure 5.** Rolling stock multibody modelled system.

The approach used to define rigid bodies involves a master node that controls the motion of all other nodes within the body, as shown in Figure 5. The rolling stock model is represented using rigid elements connected with masses and springs, reflecting the physical characteristics of the train. Two types of joints are employed: translational and spherical. The translational joints impose five degrees of freedom (DOFs) between the nodes—two for translations and three for rotations—while the rotational joints impose three relative rotations between the nodes. These constraints are implemented using the Lagrange multiplier method [19].

A key feature of the model is its ability to incorporate rail irregularities, which significantly impact ground-borne vibrations. Rail irregularities include various imperfections and deviations along the rail profile. It is important to note that the model simplifies the wheel’s behavior by excluding rotational movement, focusing instead on translational motion.

Additionally, the method proposed for modeling the continuous introduction of loads and wheel–rail irregularities in the track model involves constructing three types of nodes:

one for introducing wheel–rail irregularities and two for simulating the wheel–rail contact. These nodes are as follows (see Figure 6):

- Physical node: Represents a characteristic point of the wheel.
- Joint node: Defines the translational joint element where wheel–rail irregularities are applied, in conjunction with the physical node of the wheel.
- Master node: Defines the element through which contact between the rolling stock and the track model is introduced, in conjunction with the physical node of the wheel.

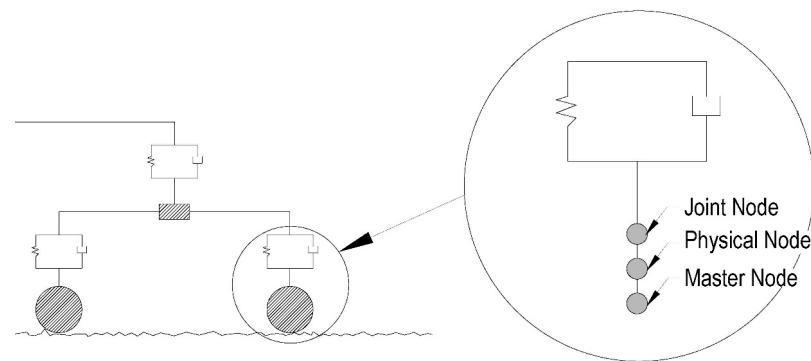


**Figure 6.** Proposed model for incorporating track defects and irregularities.

Figure 6 shows the previously described nodes.

In summary, irregularities and interaction of contact are modelled as follows:

- Modelling of wheel and rail irregularities: Achieved by incorporating a translational joint that enforces a relative displacement between the wheel and rail nodes, introducing the corresponding irregularity at each instance. This is the element between the joint node and the physical node.
- Modelling wheel–rail contact interaction: Accomplished using computational node-segment contact. This contact allows all forces or vibrations generated by the rolling stock to be transmitted to the track system, represented by the element between the physical node and the master node.

A wheel–rail roughness spectrum, which combines data from both the wheel and rail, can be used to describe the statistically consistent excitation of a specific vehicle and track. This allows for the prediction of the resulting power spectral density (PSD) of the response using random process theory [20].

The method chosen for reproducing wheel and rail irregularities, as detailed by [9], is implemented at this stage. Figure 7 shows the deflection values versus space for these surfaces. These elements are integrated into the overall mechanical system described, serving as an additional factor to consider.

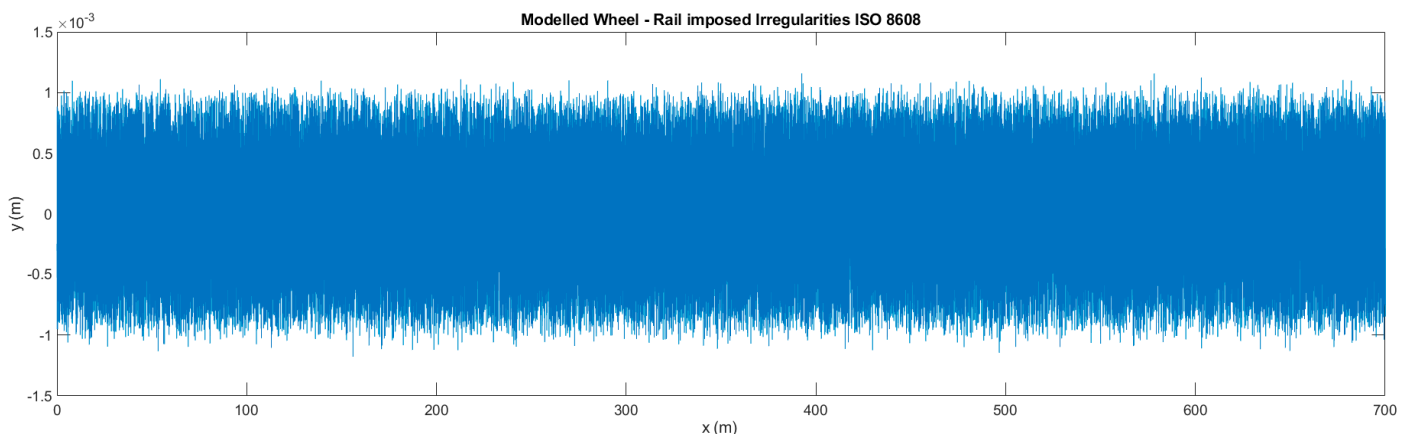


**Figure 7.** Wheel–rail model input irregularities [9].



The interaction between the train wheels and the rail is simulated using point-to-surface contact, incorporating a frictionless interface with capabilities for both sliding and separation. The contact algorithm used in this simulation is based on the augmented Lagrangian method [17].

A key aspect of this model is the use of computational contacts to accurately represent the connections within the railway system. Unlike the previously common approach of segmenting loads, which results in discontinuous representations, this method introduces a significant improvement by converting these discontinuous load representations into continuous ones. This marks a notable shift in methodology.

### 3.3. Governing Equations

To express the dynamic behavior of the railway system within the model, fundamental equations of motion and dynamic analysis techniques are employed. The system of discrete equations for a multibody system subjected to holonomic constraints is as follows [19]:

$$M(u)\ddot{u} + f(u, \dot{u}) + B^T(u)\lambda = 0 \quad (1)$$

$$C(u) = 0 \quad (2)$$

$M$  is the mass matrix, which is a function of the displacements because of the presence of rigid bodies.  $f$  is a vector, which include the effects of external forces (gravity) and internal forces from dampers.  $B$  and  $C$  are the constraint matrix and vector corresponding to the constraint equations introduced by the joints and the contact algorithm, and  $\lambda$  is the Lagrange multipliers vector. Linearization of the system of equations (Equations (3) and (4)) gives [19] the following:

$$\left( K(u, \dot{u}, \ddot{u}) + K^b(u, \lambda) \right) \Delta u + G(u, \dot{u}) \Delta \dot{u} + B^T(u) \Delta \lambda = -M(u)\ddot{u} - f(u, \dot{u}) - B^T(u)\lambda \quad (3)$$

$$K^c(u) \Delta u = -C(u) \quad (4)$$

where:

$$K = \frac{\partial (M(u)\ddot{u} + f(u, \dot{u}))}{\partial u} \quad (5)$$

$$G = \frac{\partial f(u, \dot{u})}{\partial u} \quad (6)$$

$$K^b = \frac{\partial (B^T \lambda)}{\partial u} \quad (7)$$

$$K^c = \frac{\partial C}{\partial u} \quad (8)$$

### 3.4. Loading Description

The simulation is divided into two steps. In the first step (initial stress introduction), inertia effects are not considered. This phase focuses on introducing initial stress due to the self-weight of both the terrain and rolling stock. The rolling stock is assumed to be on a rigid platform, so the terrain's stress state is solely due to gravity. This step involves a nonlinear static analysis, where geometric nonlinearity accounts for the initial deformation of the rolling stock caused by its self-weight, ensuring consistency with equilibrium stresses. In the second step (transient analysis), inertia effects are included, and a full nonlinear transient analysis is performed. This step captures the dynamic behavior of the system, considering the effects of inertia on the rolling stock and terrain.

Both steps are solved as part of the same transient analysis, with the first step focusing on static effects and neglecting dynamic effects. In this initial step, displacement and

velocity are set to zero to establish initial conditions. During the second step, dynamic effects are introduced, and velocity is applied to the master node of the traction vehicle.

The time-integration method used in the second step is the Newmark method [21]. This method assumes that:

$${}^{t+\Delta t}\dot{u} = {}^t\dot{u} + \left[ (1 - \delta) {}^t\ddot{u} + \delta {}^{t+\Delta t}\ddot{u} \right] \Delta t \quad (9)$$

$${}^{t+\Delta t}u = {}^tu + {}^t\dot{u}\Delta t + \left[ \left( \frac{1}{2} - \alpha \right) {}^t\ddot{u} + \alpha {}^{t+\Delta t}\ddot{u} \right] \Delta t^2 \quad (10)$$

where the super index  $t + \Delta t$  indicates a value at the end of a time increment, and the superindex  $t$  indicates a value at the beginning of the time increment. Time integration parameters of the Newmark method,  $\alpha$  and  $\delta$ , are expressed in terms of the amplitude decay factor  $\gamma$ , which is introduced to filter the influence of high frequencies:

$$\delta = \frac{1}{2} + \gamma \quad (11)$$

$$\alpha = \frac{1}{4}(1 + \gamma)^2 \quad (12)$$

In the present simulations, due to the high-speed vibrations, the value of  $\gamma$  used for this model is 0.005.

### 3.5. Boundary Conditions

To ensure realistic simulations, our model adheres to specific boundary conditions:

- **Symmetry conditions:** Applied along the longitudinal axis of the track, these conditions enhance computational efficiency and ensure symmetry in the model's responses.
- **Model length:** The model's minimum length is set to 84 m, as referenced in [22]. This length is crucial for accurately capturing ground-borne vibrations.

Additionally, the model incorporates a critical feature proposed by [18]. This involves placing several springs around the platform at the vertical planes of the model's beginning and end, as well as beneath the lower horizontal plane, to ensure the effective absorption of wave reflections.

By incorporating these specific boundary conditions and absorption mechanisms, the developed model achieves a robust representation of railway-induced ground vibrations. This setup enables the simulation of realistic scenarios while effectively mitigating boundary effects that might otherwise compromise the accuracy of the results. The subsequent section presents the findings from these numerical simulations.

## 4. Results and Discussion

In this section, the results obtained from the numerical model are presented, which are a valuable tool for quantifying its environmental impact and elucidating the complex dynamics of ground-borne vibrations in railway systems.

The results detail the effects observed when a train passes a specified reference point. Figure 8 illustrates the time-domain accelerations recorded along the  $y$ -axis in the rail at a specific location—the precise center of the entire model.

It is crucial to highlight that, in the displayed graph, a clear correspondence is evident between the accelerogram peaks (passing of the axles) and the central areas among them, emphasizing the geometry and load distribution of the rolling stock. This observation signifies the visible representation of the energy generated as the rolling stock passes.

The central regions between the peaks illustrate wheel and rail irregularities, as well as other movements caused by the train's motion. The smaller intermediate peaks, characterized by less energetic vibrations, serve as a representation of the enrichment introduced by the continuous modelling of the entire system. This encompasses the

implementation of a continuous system and continuous loads. As previously discussed in the literature review, the information presented here must be complementarily showcased in both the time and frequency domains to provide a comprehensive understanding of the situation.

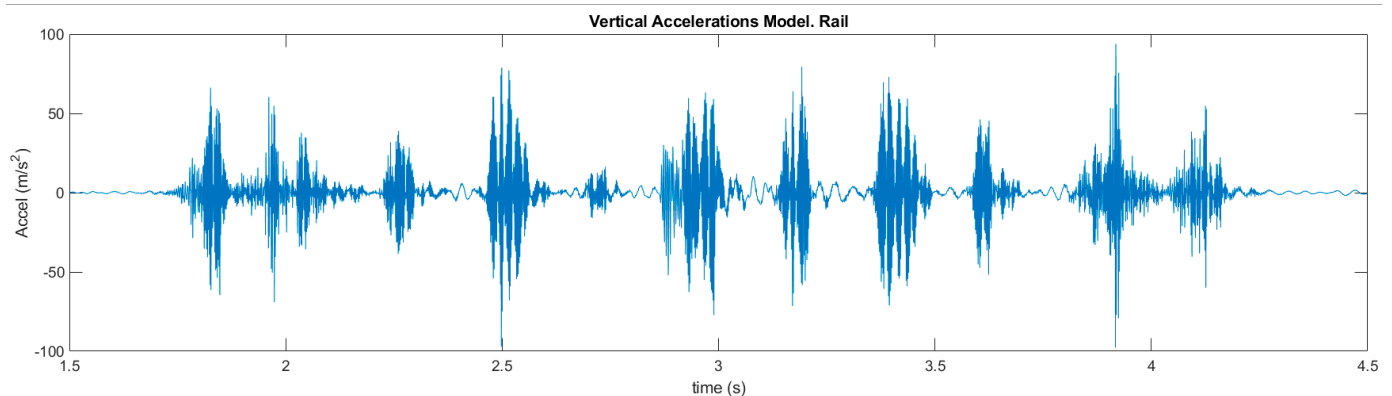


**Figure 8.** Acceleration versus time in the rail. Proposed model.

These nuanced results, complementing those obtained in the time domain, are illustrated in Figure 9. It is noteworthy that the entire spectrum is fully captured, capturing the most representative frequencies—peaks, attributed to the reduction of the time step and the continuous way of introducing the loads, with calculations fixed at a frequency of 1024 Hz—which are identical to the referenced measured vibration spectra. This translates to an average of over 4000 full-model calculations for every four seconds of simulation (1024 calculations per second), covering the entire passage of the train.

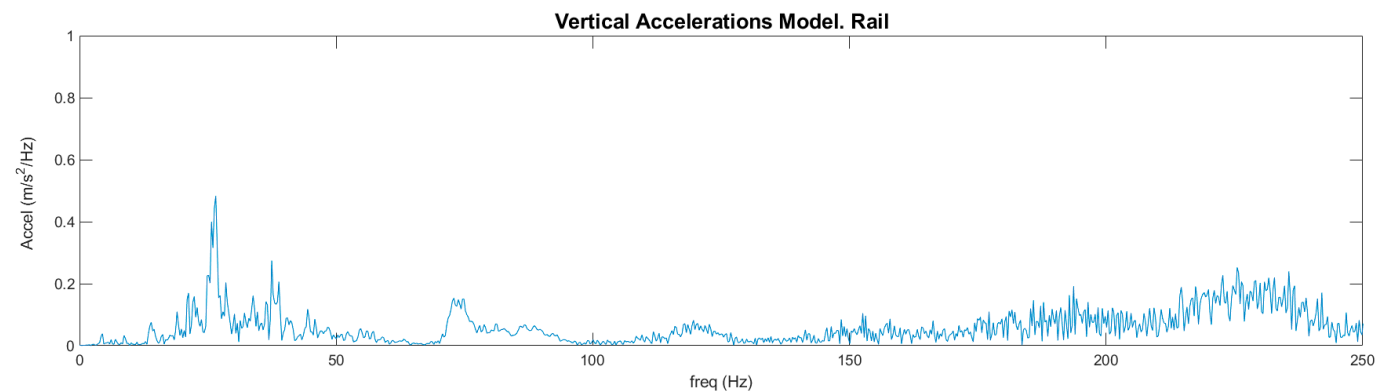


**Figure 9.** Frequency domain spectra acceleration (FFT). Proposed model.

Regarding the representation of results in the frequency domain, a comprehensive frequency representation is observed across the entire spectrum to have a complex image of the predicted phenomena. The model's groundbreaking advancements become evident in its representation of results within the frequency domain. It offers a comprehensive view across the entire spectrum, providing a nuanced understanding of predicted phenomena. These insights significantly enhance our grasp of vibrations stemming from railway operations, particularly when integrated into three-dimensional numerical models capable of accommodating various track system configurations.

The wealth of information provided by this model is indispensable for supplementing data in the time domain, especially when considering the design of specialized track components or attenuation measures to mitigate vibrational pollution. Notably, the ability to identify prominent or energetic vibrational frequencies facilitates an informed material selection for optimal effectiveness.

In essence, this model represents a significant leap forward, offering unparalleled insights that can revolutionize our approach to mitigating vibrational impacts in railway environments.

## 5. Experimental Validation

Thanks to published and discussed data [4], this model underwent validation through a comparison with a scenario similar to the conditions mentioned in the experimental data section. The validation of the model's results was carried out through direct comparison. This method of assessing results was implemented due to its widespread use in this type of predictive models by highly relevant authors in the field [8,23–29].

The objective of these predictions is not to acquire precise data in absolute terms relative to the initial data series, but rather to conform to the characteristics of the power spectral density (PSD) produced by the phenomenon of the rolling stock traversing the track. This phenomenon is inherently difficult to precisely adjust, as its most influential effect is the wheel–rail irregularity, which comprises a unique and variable signature at each spatial position of both the wheel and the rail, as irregularities are introduced statistically [20]. On-site measured data from the referenced study are depicted in Figures 10 and 11, representing the time and frequency domains, respectively.

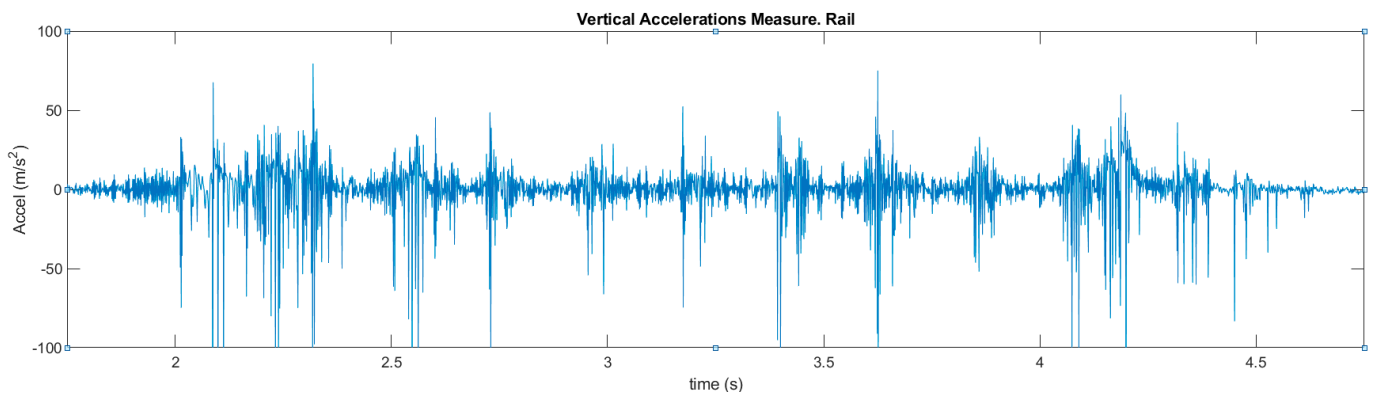


**Figure 10.** Time domain measured acceleration at 300 km/h speed passing, with data obtained from [4].

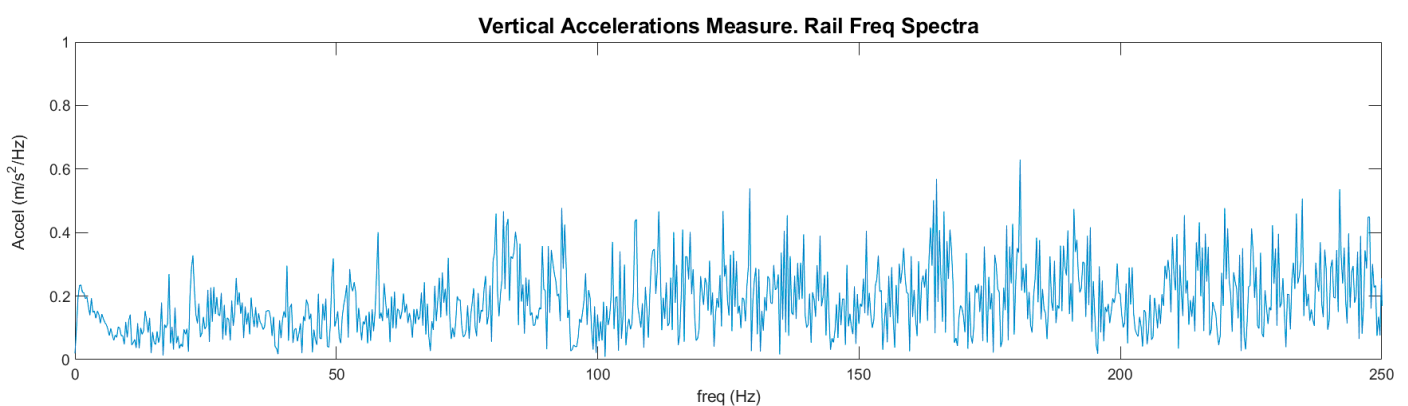


**Figure 11.** Frequency domain measured spectra acceleration (FFT) at 300 km/h speed passing, with data obtained from [4].

These presented results conclusively demonstrate that the main graph peaks share the same order of magnitude, and the passage of the axles is consistently depicted, particularly in the time domain (Figure 8 vs. Figure 10). This signifies that the simulated values align closely with the experimental on-site measurements, establishing the presented model as validated. Shifting to the frequency domain, the entire spectrum is encompassed by the

assumed standardized wheel–rail unevenness, which is generic. This successful coverage affirms the correctness and effectiveness of the employed method in this domain.

Additionally, Figure 12 is presented below to provide a comparison of the data in both the time and frequency domains, offering a more robust validation of the model's performance.

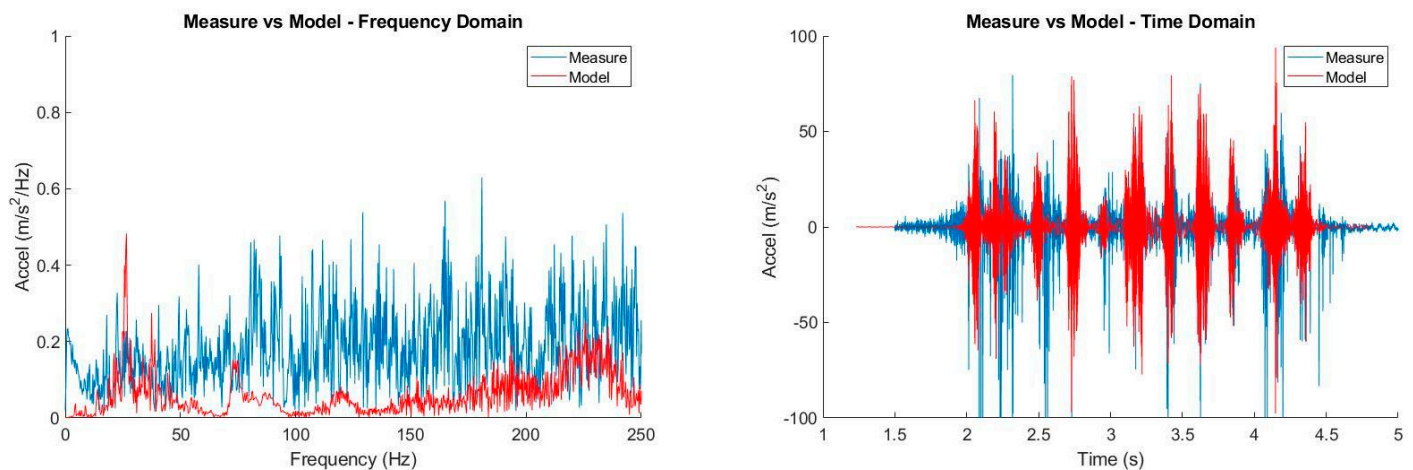


**Figure 12.** Comparison between the model results and actual measurements in both the frequency domain (left) and the time domain (right). Real data were measured at 300 km/h, with data obtained from [4].

## 6. Conclusions

These deductions are obtained from rigorous simulations and meticulous data analyses obtained from the analyzed bibliography. These findings shed light on the complex interplay between the rolling stock, track components, and surrounding environment, ultimately enhancing our understanding of the factors contributing to ground-borne vibrations. Through these results, we embark on a journey to untangle the intricacies of railway-induced vibrations, paving the way for informed decision making and effective mitigation strategies.

The main conclusions of this article could be grouped by the following statements:

- Continuity in load representation has yielded substantial benefits, particularly in the faithful depiction of frequency characteristics, as shown in the Results section.
- Advancements in frequency domain accuracy: A pivotal outcome of our research is the substantial enhancement of numerical models, particularly in the frequency domain.
- The accurate representation of measured data signifies a significant advancement in railway engineering, facilitating more dependable assessments and predictions of ground-borne vibrations caused by train operations.
- This approach facilitates a thorough depiction of phenomena from the source through the entire track system, enabling the effective simulation of various elements' influence so as to attenuate these vibrations.
- The model's proficiency in capturing frequency-specific data offers a profound understanding of the vibrational characteristics linked to railway-induced ground vibrations.
- This model is capable of quantifying environmental effects, which is essential to allow the precise planning and assessment of future railway infrastructures, their vibrational emissions, and their overall sustainability.
- A possible limitation of this model mainly stems from its dependency on rail irregularities, which have been identified as the most influential factor in the frequency domain.

In summary, transitioning from discontinuous to continuous load simulations, our model enhances the precision of frequency representations, providing a more comprehensive and accurate assessment of ground-borne vibrations induced by railway operations. The advancements made in the presented numerical model and the seamless integration

between time and frequency domains stand as a testament to the strides taken toward more accurate, sustainable, and resilient railway infrastructures.

## 7. Further Developments

These findings hold immense promise for the future planning and design of railway systems, paving the way for more efficient and environmentally conscious transportation networks. Some potential areas for further development could include:

- Utilization of advanced models in railway superstructure design: The utilization of these advanced numerical models holds promise in designing future railway superstructures, leading to more robust and vibration-resilient railway infrastructures.
- Improved sustainability assessment and design metrics: This enhanced index holds the potential to serve as a cornerstone for evaluating sustainability aspects in railway construction, enabling better-informed decisions and more sustainable infrastructure designs.
- A possibility to study the influence of the quality of track maintenance and rolling stock wheels, with a focus on different scenarios using actual measured rail irregularity data, preferably obtained directly from track measurements, to further enhance the model's accuracy and applicability.

**Author Contributions:** Conceptualization, A.G.M., I.J.T. and J.J.R.A.; data curation, A.G.M.; formal analysis, A.G.M. and A.A.L.; funding acquisition, J.J.R.A.; investigation, A.G.M. and J.J.R.A.; methodology, A.G.M., A.A.L., M.G.C.G., I.J.T. and J.J.R.A.; project administration, I.J.T. and J.J.R.A.; resources, I.J.T. and J.J.R.A.; software, A.G.M. and A.A.L.; supervision, I.J.T. and J.J.R.A.; validation, A.G.M. and A.A.L.; writing—original draft, A.G.M. and J.J.R.A.; writing—review and editing, M.G.C.G., I.J.T. and J.J.R.A. All authors have read and agreed to the published version of the manuscript.

**Funding:** This research received no funding.

**Data Availability Statement:** Measured data from [4] is available at the following link: <https://bwk.kuleuven.be/bwm/research/L1measurements>.

**Acknowledgments:** This research has been made possible through a collaboration with the University of Cadiz, specifically with the intensive involvement Intelligent Modelling of Systems research group.

**Conflicts of Interest:** The authors declare no conflicts of interest.

## References

1. Gupta, S.; Fiala, P.; Hussein, M.F.M.; Chebli, H.; Degrande, G.; Augusztinovicz, F.; Hunt, H.E.M.; Clouteau, D. A Numerical Model for Ground-Borne Vibrations and Reradiated Noise in Buildings from Underground Railways. In Proceedings of the ISMA2006: International Conference on Noise and Vibration Engineering, Leuven, Belgium, 17–19 September 2006; Volume 3, pp. 1741–1755.
2. Garcia Moreno, A.; Ruiz Aguilar, J.J.; Moscoso Lopez, J.A. Towards the Numerical Ground-Borne Vibrations Predictive Models as a Design Tool for Railway Lines: A Starting Point The. *Transp. Res. Procedia* **2021**, *58*, 363–369. [CrossRef]
3. Yaseri, A.; Baziyar, M.H.; Hataf, N. 3D Coupled Scaled Boundary Finite-Element/Finite-Element Analysis of Ground Vibrations Induced by Underground Train Movement. *Comput. Geotech.* **2014**, *60*, 1–8. [CrossRef]
4. Degrande, G.; Schillemans, L. Free Field Vibrations during the Passage of a Thalys High-Speed Train at Variable Speed. *J. Sound Vib.* **2001**, *247*, 131–144. [CrossRef]
5. Auersch, L. Ground Vibration Due to Railway Traffic-The Calculation of the Effects of Moving Static Loads and Their Experimental Verification. *J. Sound Vib.* **2006**, *293*, 599–610. [CrossRef]
6. Galvín, P.; Domínguez, J. High-Speed Train-Induced Ground Motion and Interaction with Structures. *J. Sound Vib.* **2007**, *307*, 755–777. [CrossRef]
7. Lombaert, G.; Degrande, G. Ground-Borne Vibration Due to Static and Dynamic Axle Loads of InterCity and High-Speed Trains. *J. Sound Vib.* **2009**, *319*, 1036–1066. [CrossRef]
8. Lombaert, G.; Galvín, P.; François, S.; Degrande, G. Quantification of Uncertainty in the Prediction of Railway Induced Ground Vibration Due to the Use of Statistical Track Unevenness Data. *J. Sound Vib.* **2014**, *333*, 4232–4253. [CrossRef]
9. ISO8608 (BS7853:1996); Mechanical Vibration—Road Surface Profiles—Reporting of Measure Data. International Organization for Standardization (ISO): Geneva, Switzerland, 1995.
10. Romero, A.; Galvín, P.; Domínguez, J. 3D Non-Linear Time Domain FEM-BEM Approach to Soil-Structure Interaction Problems. *Eng. Anal. Bound. Elem.* **2013**, *37*, 501–512. [CrossRef]

11. Sayeed, M.A.; Shahin, M.A. Dynamic Response Analysis of Ballasted Railway Track–Ground System under Train Moving Loads Using 3D Finite Element Numerical Modelling. *Transp. Infrastruct. Geotechnol.* **2022**, *10*, 639–659. [[CrossRef](#)]
12. Paul de Vos, S. *UIC Railway Induced Vibration—State of the Art Report*; International Union of Railways: Paris, France, 2017; ISBN 9782746126633.
13. Kouroussis, G.; Connolly, D.P.; Verlinden, O. Railway-Induced Ground Vibrations—A Review of Vehicle Effects. *Int. J. Rail Transp.* **2014**, *2*, 69–110. [[CrossRef](#)]
14. Zeng, Q.; Stoura, C.D.; Dimitrakopoulos, E.G. A Localized Lagrange Multipliers Approach for the Problem of Vehicle-Bridge-Interaction. *Eng. Struct.* **2018**, *168*, 82–92. [[CrossRef](#)]
15. Wang, L.; Wang, P.; Wei, K.; Dollevoet, R.; Li, Z. Ground Vibration Induced by High Speed Trains on an Embankment with Pile-Board Foundation: Modelling and Validation with in Situ Tests. *Transp. Geotech.* **2022**, *34*, 100734. [[CrossRef](#)]
16. Galvín, P.; François, S.; Schevenels, M.; Bongini, E.; Degrande, G.; Lombaert, G. A 2.5D Coupled FE-BE Model for the Prediction of Railway Induced Vibrations. *Soil. Dyn. Earthq. Eng.* **2010**, *30*, 1500–1512. [[CrossRef](#)]
17. Laursen, T.A. Computational Contact and Impact Mechanics. In *Fundamentals of Modeling Interfacial Phenomena in Nonlinear Finite Element Analysis*, 1st ed.; Springer: Berlin/Heidelberg, Germany, 2003; ISBN 978-3-540-42906-7.
18. Kouroussis, G.; Van Parys, L.; Conti, C.; Verlinden, O. Using Three-Dimensional Finite Element Analysis in Time Domain to Model Railway-Induced Ground Vibrations. *Adv. Eng. Softw.* **2014**, *70*, 63–76. [[CrossRef](#)]
19. Bachau, O.A. *Georgia I. of T. Flexible Multibody Dynamics*; Gladwell, G.M.L., Ed.; Springer: Atlanta, GA, USA, 2011; ISBN 978-94-007-0335-3.
20. Talbot, J.P.; Hunt, H.E.M. Computational Tools for Predicting Ground Vibration from Railways. In *Ground Vibrations from High-Speed Railways*; Emerald Publishing Limited: Bradford, UK, 2019; pp. 77–95.
21. Bathe, K.J. *Finite Element Procedures*, 1996th ed.; William, S., Peterson, M., Eds.; Prentice Hall: Hoboken, NJ, USA, 1996; ISBN 0-13-301458-4.
22. Galvín, P.; Domínguez, J. Analysis of Ground Motion Due to Moving Surface Loads Induced by High-Speed Trains. *Eng. Anal. Bound. Elem.* **2007**, *31*, 931–941. [[CrossRef](#)]
23. Auersch, L. The Effect of Critically Moving Loads on the Vibrations of Soft Soils and Isolated Railway Tracks. *J. Sound Vib.* **2008**, *310*, 587–607. [[CrossRef](#)]
24. López-Mendoza, D.; Romero, A.; Connolly, D.P.; Galvín, P. Scoping Methodology to Assess Induced Vibration by Railway Traffic in Buildings. *Procedia Eng.* **2017**, *199*, 2717–2722. [[CrossRef](#)]
25. Kouroussis, G.; Verlinden, O. Prediction of Railway Ground Vibrations: Accuracy of a Coupled Lumped Mass Model for Representing the Track/Soil Interaction. *Soil. Dyn. Earthq. Eng.* **2015**, *69*, 220–226. [[CrossRef](#)]
26. Kouroussis, G.; Connolly, D.P.; Vogiatzis, K.; Verlinden, O. Modelling the Environmental Effects of Railway Vibrations from Different Types of Rolling Stock: A Numerical Study. *Shock. Vib.* **2015**, *2015*, 142807. [[CrossRef](#)]
27. Kouroussis, G.; Connolly, D.P.; Olivier, B.; Laghrouche, O.; Costa, P.A. Railway Cuttings and Embankments: Experimental and Numerical Studies of Ground Vibration. *Sci. Total Environ.* **2016**, *557–558*, 110–122. [[CrossRef](#)]
28. Xu, L.; Zhai, W. A Novel Model for Determining the Amplitude-Wavelength Limits of Track Irregularities Accompanied by a Reliability Assessment in Railway Vehicle-Track Dynamics. *Mech. Syst. Signal Process* **2017**, *86*, 260–277. [[CrossRef](#)]
29. Bian, X.; Jiang, H.; Chang, C.; Hu, J.; Chen, Y. Track and Ground Vibrations Generated by High-Speed Train Running on Ballastless Railway with Excitation of Vertical Track Irregularities. *Soil. Dyn. Earthq. Eng.* **2015**, *76*, 29–43. [[CrossRef](#)]

**Disclaimer/Publisher’s Note:** The statements, opinions and data contained in all publications are solely those of the individual author(s) and contributor(s) and not of MDPI and/or the editor(s). MDPI and/or the editor(s) disclaim responsibility for any injury to people or property resulting from any ideas, methods, instructions or products referred to in the content.